

Published in final edited form as:

Eur J Med Chem. 2014 October 6; 85: 517–525. doi:10.1016/j.ejmech.2014.08.022.

Heck products of parthenolide and melampomagnolide-B as anticancer modulators that modify cell cycle progression

Narsimha R. Penthala^a, Shobanbabu Bommagani^a, Venumadhav Janganati^a, Kenzie B. MacNicol^b, Chad E. Cragle^b, Nikhil R. Madadi^a, Linda L. Hardy^b, Angus M. MacNicol^{b,*}, and Peter A. Crooks^{a,*}

^aDepartment of Pharmaceutical Sciences, College of Pharmacy, University of Arkansas for Medical Sciences, Little Rock, AR 72205, USA.

^bDepartment of Neurobiology and Developmental Sciences, University of Arkansas for Medical Sciences, Little Rock, AR 72205, USA.

Abstract

(*E*)-13-(Aryl/heteroaryl)parthenolides (**5a–i** and **6a–i**) were synthesized and evaluated for their ability to modify cell cycle progression during progesterone-stimulated *Xenopus* oocyte maturation and screened for their anticancer activity against a panel of 60 human cancer cell lines. (*E*)-13-(4-aminophenyl) parthenolide (**5b**) caused a significant inhibition of progesterone-stimulated oocyte maturation, and was determined to function downstream of MAP kinase signaling, but upstream of the activation of the universal G₂/M regulator, M-phase promoting factor (MPF, cyclin B/Cyclin-dependent kinase (CDK)). The compound (*E*)-13-(2-bromophenyl)parthenolide (**5c**) activates oocyte maturation independently of progesterone stimulation. Compounds **5b** and **5c** displayed modest growth inhibition on select cancer cell lines at 10 micromolar dose when tested on the panel of 60 cancer cell lines. By contrast, compounds (**5f** and **7**) did not modulate oocyte maturation but did exhibit micromolar level growth inhibition against most of the human cancer cell lines over a range of doses. Together, our findings indicate that screening of compounds in the oocyte maturation assay may identify additional effective cell cycle regulatory compounds that do not necessarily exert overt cytotoxicity as assessed in traditional drug screening assays.

Keywords

Parthenolide; Melampomagnolide B; Heck reaction; Oocyte maturation; Anti-cancer activity

© 2014 Elsevier Masson SAS. All rights reserved.

*Corresponding author. Tel.: +1-501-686-6495; fax: +1-501-686-6057; pacrooks@uams.edu; Angus M. MacNicol: Tel.: +1-501-296-1549; Angus@uams.edu.

Publisher's Disclaimer: This is a PDF file of an unedited manuscript that has been accepted for publication. As a service to our customers we are providing this early version of the manuscript. The manuscript will undergo copyediting, typesetting, and review of the resulting proof before it is published in its final citable form. Please note that during the production process errors may be discovered which could affect the content, and all legal disclaimers that apply to the journal pertain.

1. Introduction

Parthenolide (PTL, **1**) is a naturally occurring sesquiterpene lactone, isolated from *Tanacetum parthenium* (feverfew), which is used in the treatment of fever, migraine headaches, rheumatoid arthritis, and also as an anti-inflammatory agent [1–3]. In recent years the PTL molecule and several structurally related sesquiterpene lactone analogs have been extensively studied because of their potent anti-tumor and cytotoxic properties [4–12]. The presence of the α -methylene- γ -lactone moiety in these compounds was reported to be essential for their cytotoxic activity [13, 14], inhibition of NF- κ B [15] and antitumor properties [16, 17]. The *exo*-methylene moiety was regarded as important because of its exceptional reactivity towards nucleophilic functional groups [14]. PTL has been shown to target NF- κ B, Stat3, HDAC, SERCA, and COX-2 in cancer cells [18–21]. Despite promising *in vitro* activity, this potent natural product has a major limitation which prevents its further development as a therapeutic agent, that is, its poor water-solubility (0.169 μ mol/mL maximum solubility in serum) and poor oral bioavailability, thus limiting its potential as a promising clinical agent [22, 23].

PTL has become a key source of several novel antileukemic compounds over the past decade. From our research on antileukemic analogs of PTL, we resolved the poor water-solubility issue by addition of polar, protonatable amine moieties to the exocyclic methylenide group via Michael addition chemistry. These amine adducts were then able to be converted to stable, water-soluble salts [23–26]. Guzman *et al.* have reported that one such PTL derivative induces robust apoptosis of primary acute myeloid leukemia (AML) stem and progenitor cells *in vitro*, with minimal toxicity towards normal hematopoietic stem cells [24, 25]. Specifically, a Michael adduct of PTL (**1**), dimethylaminoparthenolide (DMAPT, **2**), exhibited antileukemic efficacy against primary leukemia AML stem cells, and had low toxicity and 70% oral bioavailability in preclinical studies. DMAPT has progressed to phase-I clinical trials in the United Kingdom for the treatment of AML, ALL, and CLL [25]. The PTL structure can be chemically modified to afford a variety of structural scaffolds, such as guaianolides, pseudoguaianolides, germacrolides, melampolides, heliangolides, and 4,5-dihydro-germacranolides [27]. Based on this, in an earlier communication we reported the synthesis and anti-leukemic activity of a melampolide sesquiterpene lactone, melampomagnolide-B (MMB, **3**) [28]. In the present work, we focus on the synthesis of novel *E*-olefinic coupled products of both PTL and MMB utilizing Heck reaction conditions [29]. These molecules represent new, protectable sesquiterpene scaffolds with novel biological properties, and their general method of preparation allows diverse structural modification amenable to both biological and physico-chemical optimization via structure-activity studies (SAR) and structure-property studies (SPR). These Heck products have been screened for their effects on cell cycle progression during *Xenopus* oocyte maturation and for their *in vitro* anti-cancer activity against the panel of 60 human cancer cell lines.

2. Chemistry

Novel *E*-olefinic coupling products of PTL (**5a–h**, Table 1) were prepared under Heck reaction conditions utilizing palladium ferrocene [Pd(dppf)Cl₂] as a catalyst in toluene and

heating the mixture with an appropriate iodo-aromatic or iodo-heteroaromatic compound in the presence of di-isopropylethylamine (DPEA) as base (Scheme 1). Previously, this reaction has been carried out using palladium (II) acetate as catalyst [29]; however, we have observed that the replacement of palladium acetate by palladium (II) ferrocene catalyst affords significantly improved yields of Heck product.

The above Heck products were converted to their respective MMB analogs (**6a–h**, Table 1) by utilizing selenium dioxide/*t*-butyl hydroperoxide as oxidizing reagent [28]. The structure and purity of these derivatives was verified by ¹H and ¹³C-NMR spectroscopy. Single crystal X-ray crystallographic data confirmed the double bond geometry of the resulting oxidized products [30]. When PTL (**1**) was reacted with 2-iodoimidazole (**4i**) in the presence of Pd(dppf)Cl₂ catalyst in dimethyl formamide the desired Heck *E*-olefinic product **5i** was not obtained, due to PTL undergoing a Michael addition to afford compound **7**, which has been previously prepared in our laboratory under Michael reaction conditions [23]. Compound **7** prepared under Heck reaction conditions was shown to have identical structural properties (¹H and ¹³C NMR data) as **7** prepared under Michael reaction conditions [23, 26]. Compound **7** was subsequently converted to its MMB analog **8** via oxidation with SeO₂/*t*-BuOOH, as shown in Scheme 2.

3.0. Anti-cancer activity

3.1. *Xenopus* bio-assay

Xenopus Dumont Stage VI oocytes are arrested at the G₂/M border of the cell cycle and in response to the steroid hormone, progesterone, re-enter the cell cycle and proceed to metaphase of meiosis II, at which point they undergo cell cycle arrest. These mature oocytes are competent to be fertilized by sperm. Progression through oocyte maturation occurs in the absence of gene transcription [31, 32], relies on sequential activation of distinct mRNA translational control pathways, and is regulated by action of the evolutionarily conserved CDK and MAP kinase (MAPK) signaling pathways [33]. Morphologically, progesterone stimulation results in the appearance of a white spot on the dark animal hemisphere indicative of germinal vesicle (nuclear) breakdown (GVBD). We have recently employed *Xenopus* oocyte maturation to assess the cell cycle regulatory properties of a novel set of heterocyclic aminoparthenolide derivatives [34]. Here, we employ the oocyte assay to assess the biological activity of a series of novel PTL and MMB analogs, and to position bioactive compounds within the well-characterized oocyte signal transduction pathways.

The above (*E*)-13-(aryl/hetero aryl)-parthenolide analogs and their MMB derivatives, were screened for their effects in *Xenopus* oocyte maturation bioassays (Fig. 2). *Xenopus* oocytes were isolated and cultured as described previously [35]. The oocytes were induced to mature at a concentration of 2 μg/ml progesterone [36] and the rate to GVBD was scored. Because oocytes from different frogs mature at different rates in response to progesterone, the culture times were standardized between experiments to the time taken for 50% of oocytes to undergo GVBD (designated GVBD₅₀). As indicated, oocytes were pre-treated with test compounds or DMSO vehicle overnight, prior to progesterone addition.

Several compounds were identified that reproducibly inhibited or activated maturation. Of these, the 4-aminophenyl analog (**5b**) attenuated progesterone-dependent oocyte maturation when tested at an initial test dose of 100 μM relative to DMSO-vehicle-treated control oocytes (Fig. 3). This attenuation was due to a delay, rather than an overt block to progesterone-induced maturation, and occurred over a range of doses (Fig. 4). When assayed over 5 independent experiments, **5b** was found to have an EC_{50} of 5 μM (Fig. 5). To assess the possible point of action of **5b**, time-match protein lysates were prepared from DMSO- or **5b**-treated oocytes that had been stimulated with progesterone, when 50% of the DMSO-treated oocytes completed GVBD (GVBD_{50}).

As can be seen in Fig. 6, phosphorylation and activation of MAPK occurred normally in both sample sets. However, **5b**-treated oocytes failed to dephosphorylate and activate the *cdc2* catalytic component of universal G_2/M regulator, M-phase promoting factor (MPF, cyclin B/cyclin-dependent kinase (CDK)). Thus, **5b** appears to function to attenuate oocyte cell cycle progression downstream of MAP kinase, but upstream of CDK dephosphorylation. Of note, the MMB Heck analog **6b**, failed to modulate oocyte cell cycle progression.

The 2-bromophenyl analog **5c** triggered progesterone-independent maturation. When assessed over three independent experiments, **5c** functioned with an EC_{50} of 6 μM (Fig. 7). To assess where **5c** was functioning within the oocyte maturation process, oocytes were treated with DMSO (vehicle) or compound **5c** and harvested when 50% of the **5c** treated oocytes completed GVBD. The **5c** treated oocytes were then segregated into those that had not (-) or had (+) completed GVBD. When examined by western blotting, compound **5c** triggered progesterone-independent activation of MAPK, the dephosphorylation of *cdc2* and activation of MPF. MAPK activation preceded GVBD, while *cdc2* activation occurred predominantly at GVBD (Fig. 8). It remains to be determined if the action of **5c** on MAPK (Fig. 8) is through direct or indirect mechanisms. Indeed, future studies will be necessary to determine the precise point of action of **5b** and **5c**.

3.2. Anti-cancer activity against human cancer cell lines in culture

The (*E*)-13-(aryl/hetero aryl)parthenolides (**5a-h**) and their MMB analogs (**6a-h**) were screened against a panel of 60 human cancer cell lines. Initial screening was carried out at a single concentration (10^{-5} M). Compound **5b** caused modest growth inhibition of MOLT-4 leukemia cells and PC-3 prostate cancer cells (24.23% and 20.51% inhibition, respectively) but was not particularly effective against the other cell lines in the panel. Compound **5c** caused modest growth inhibition of leukemia cells (CCRF-CEM: 22.33%; HL-60(TB): 34.11%; K562: 28.06%; MOLT-4: 31.19%; and RPMI-8226: 21.31%), as well as PC-3 prostate cancer cells (42.28%) and MCF-7 breast cancer cells (24.31%). Compound **6c**, the MMB derivative of **5c**, induced progesterone-independent oocyte maturation (Fig. 2), was more soluble than **5c** but had reduced efficacy in the NCI 60 panel where it attenuated growth of only CCRF-CEM leukemic cells (28.48% inhibition) and BT-549 breast cancer cells (24.21% inhibition).

Compounds **5f** and **7** exhibited more than 60% growth inhibition in at least eight cell lines from the panel of sixty cell lines, and were selected for multiple dose studies at five different concentrations (10^{-4} M, 10^{-5} M, 10^{-6} M, 10^{-7} M and 10^{-8} M). Dose-response curves were created by plotting cytotoxic effect against the \log_{10} of the drug concentration for each cell line. Cytotoxic effects of each compound were determined as GI_{50} , and LC_{50} values, which represent the molar drug concentration required to cause 50% growth inhibition, and the concentration that kills 50% of the cells, respectively. The results are presented in Table 2.

The thiophene-3-yl analog **5f** exhibited growth inhibitory properties against all cancer cell lines in the panel, with GI_{50} values in the range of 5.44 to 48.1 μ M (Table 2) and exhibited growth inhibitory activity against NCI-H522 non-small cell lung cancer cells ($GI_{50}=5.44\mu$ M; $LC_{50}=59.7\mu$ M), leukemia CCRF-CEM ($GI_{50}=19.1\mu$ M; $LC_{50}\Rightarrow 100\mu$ M) and RPMI-8226 ($GI_{50}=19.7\mu$ M; $LC_{50}\Rightarrow 100\mu$ M) cancer cells lines, CNS SF-539 ($GI_{50}=16.1\mu$ M; $LC_{50}\Rightarrow 62.2\mu$ M), melanoma UACC-62 ($GI_{50}=13.8\mu$ M; $LC_{50}=76.6\mu$ M), SK-MEL-5 ($GI_{50}=16.3\mu$ M; $LC_{50}=60.4\mu$ M), renal A498 ($GI_{50}=17.5\mu$ M; $LC_{50}\Rightarrow 100\mu$ M), and breast cancer MDA-MB-231/ATCC ($GI_{50}=16.0\mu$ M; $LC_{50}=81.8\mu$ M) cancer cell lines.

The 2-imidazole Michael adduct **7** exhibited growth inhibitory properties against all but one of the cancer cell lines in the panel, with GI_{50} values in the range of 1.71 to 47.4 μ M (Table 2). Notably, compound **7** exhibited significant growth inhibitory activity against NCI-H522 non-small cell lung cancer cells ($GI_{50}=1.77\mu$ M; $LC_{50}=6.34\mu$ M), and leukemia CCRF-CEM cell lines ($GI_{50}=6.13\mu$ M; $LC_{50}=79.6\mu$ M).

4.0. Conclusions

The frog *Xenopus* has a unique combination of evolutionary relatedness to humans and experimental malleability that have engendered fundamental insights into vertebrate cellular and developmental biology. The dependence of *Xenopus* oocyte maturation and early embryonic development on regulated protein synthesis provides a rapid and powerful bioassay to identify small molecule compounds that impinge on cell cycle progression in a transcription-independent cellular environment. In this study we identify several bioactive PTL derivatives that exert profound effects on G_2/M cell cycle progression. The 4-aminophenyl analogue (**5b**) attenuated progesterone-dependent maturation and functioned downstream of MAP kinase activity and upstream of cyclin B/CDK activation. By contrast, the 2-bromophenyl moiety (**5c**) induced progesterone-independent oocyte maturation. Consistent with these compounds targeting conserved cellular entities, both **5b** and **5c** had modest, but significant growth inhibitory effects on a select subset of human cancer cell lines in the NCI 60 human cancer cell panel. While growth inhibitory effects of **5b** may have been predicted, based on the attenuation of MPF activation, the growth inhibitory mechanism of **5c** remains to be determined. With the exception of **6c**, the MMB Heck reaction analogs (**6a-h**) did not show any effect on oocyte maturation. The thiophene-3-yl analog **5f**, and the 2-iodo- imidazole analog **7** were identified as being efficacious in the 60 cancer cell panel screen. However, neither of these molecules modulated *Xenopus* oocyte maturation. This suggests that they may not inhibit within the G_2/M phase of the cell cycle, or that they target a transcription-dependent growth inhibitory process. Together, our data indicate that screening of small molecules for modulation of *Xenopus* oocyte cell cycle

progression may complement screening of such molecules in the human cancer cell panel to identify novel compounds that may be advantageous for drug development for treatment of human cancer.

In summary, we report the synthesis of several new PTL and MMB derivatives and have identified several compounds with anticancer activity against a panel of human cancer cell lines. Future studies will determine the cellular targets of action of these novel bioactive molecules.

5.0. Experimental section

5.1. Chemistry

General Information: Melting points were recorded on a Fisher scientific apparatus and are uncorrected. TLC controls were carried out on precoated silica gel plates (F 254 Merck). IR spectra were recorded on a Thermo scientific OMNIC FTIR spectrometer. ^1H and ^{13}C NMR spectra were obtained on an Agilent 400 MHz spectrometer equipped with a Linux workstation running on vNMRj software package. All the spectra were phased, baseline was corrected where necessary, and solvent signals (CDCl_3) were used as reference for both ^1H and ^{13}C spectra. The chemical shifts are expressed as δ values in parts per million (*ppm*) and the coupling constants (*J*) are given in hertz (Hz). Accurate mass data were obtained on an Agilent 6210 LCTOF instrument operated in the multimode condition (ESI/APCI). Samples were introduced via a flow injection system using methanol (95%), water (5%) containing 0.1% formic acid. The fragmentor voltage was 115v, charging voltage 2000v, and nebulizing gas and drying gas were both at 200 °C.

5.1.0. General synthetic procedure for C-C bond formation (5a–h)—A mixture of parthenolide (1.0 mmol) and an appropriate aromatic iodide (1.1 mmol) was refluxed at 80 °C using palladium (II) ferrocene (0.01 mmol) and di-isopropylethylamine (3.0 mmol) in toluene (0.1 ml) under air for 18–24 h. The reaction mixture was then allowed to cool to room temperature, water (8 ml) added, and the resultant mixture was extracted with ethyl acetate (10ml \times 3). The separated organics were dried over Na_2SO_4 , filtered and the filtrate concentrated under reduced pressure. The obtained crude residue was purified by silica flash chromatography (9:1 to 4:1, hexanes/EtOAc) to afford the corresponding aryl substituted parthenolide as a solid (40–50 mg) in 70 to 80 % yield.

5.1.1. Synthesis of (E)-13-(4-aminophenyl)parthenolide (5b)—Light yellow solid; mp: 239–241 °C; IR: 3353.61, 2915.89, 2850.32, 1720.22, 1608.37, 1591.01, 1515.80, 1436.41, 1380.80, 1299.81, 1267.02, 1193.24, 1162.81, 1064.53, 1000.89, 914.04, 873.61, 823.47, 806.11, 746.3, 674.97, 638.33 cm^{-1} ; ^1H NMR (400 MHz, CDCl_3): δ 7.54 (d, *J* = 2.8 Hz, 1H, 13-CH), 7.24 (d, *J* = 8.4 Hz, 2H, Ar-H), 6.69 (d, *J* = 8.0 Hz, 2H, Ar-H), 5.29 (d, *J* = 11.2 Hz, 1H, 1-CH), 4.02 (brs, 2H, NH_2), 3.93 (t, *J* = 8.0 Hz, 1H, 6-CH), 3.25 (d, *J* = 2.8 Hz, 1H, 5-CH), 2.83 (t, *J* = 8.8 Hz, 1H, 7-CH), 2.28–2.45 (m, 1H, 2-CH), 2.14–2.24 (m, 5H, 2-CH, 9- CH_2 , 3-CH, 8-CH), 1.69 (s, 3H, 14- CH_3), 1.61 (s, 1H, 3-CH), 1.43–1.45 (m, 1H, 8-CH), 1.31 (s, 3H, 15- CH_3) *ppm*; ^{13}C NMR (100 MHz, CDCl_3): δ 171.63, 148.15, 138.64, 134.79, 132.17, 125.12, 124.03, 123.29, 114.42, 82.71, 66.62, 61.58, 46.98, 41.88, 36.10,

29.33, 24.33, 17.49, 17.36 ppm. HRMS calcd for C₂₁H₂₆NO₃, (M+H)⁺: 340.1913 Found 340.1921.

5.1.2. Synthesis of (E)-13-(2-bromophenyl)parthenolide (5c)—White solid; mp: 230–231 °C; IR: 2960.12, 2925.25, 1758.79, 1648.87, 1629.58, 1467.59, 1417.56, 1317.16, 1288.24, 1278.59, 1240.02, 1209.14, 1193.74, 1172.53, 1024.21, 998.24, 912.18, 871.68, 800.33, 767.54, 671.12, 628.69 cm⁻¹; ¹H NMR (400 MHz, CDCl₃): δ 7.76 (d, *J* = 3.6 Hz, 1H, 13-CH), 7.66 (d, *J* = 7.6 Hz, 1H, Ar-H), 7.37 (m, 2H, Ar-H), 7.25 (m, 1H, Ar-H), 5.35 (d, *J* = 10.4 Hz, 1H, 1-CH), 3.97–3.93 (q, *J* = 16.0, 7.2 Hz, 1H, 6-CH), 3.24 (d, *J* = 3.6 Hz, 1H, 5-CH), 2.82 (d, *J* = 8.8 Hz, 1H, 7-CH), 2.43–2.38 (q, *J* = 18.0 Hz, 1H, 9-CH), 2.23–2.15 (m, 2H, 2-CH₂), 1.96–1.94 (m, 9H, 2-CH, 3-CH), 1.86–1.81 (m, 1H, 8-CH), 1.63 (s, 3H, 14-CH₃), 1.39–1.25 (m, 5H, 15-CH₃, 3-CH, 8-CH) ppm; ¹³C NMR (100 MHz, CDCl₃): δ 171.03, 136.94, 134.85, 134.6, 133.16, 131.81, 130.63, 129.4, 127.04, 124.7, 124.52, 83.02, 66.6, 61.5, 46.6, 41.3, 36.2, 30.06, 24.1, 17.3, 17.2 ppm. HRMS calcd for C₂₁H₂₄BrO₃, (M+H)⁺: 403.0909 Found 403.0917.

5.1.3. Synthesis of (E)-13-(4-fluorophenyl)parthenolide (5d)—White solid; mp: 269–271 °C; IR: 3031.60, 2931.32, 1749.15, 1660.44, 1648.87, 1591.01, 1552.44, 1517.73, 1411.66, 1349.95, 1332.59, 1249.67, 1232.31, 1209.24, 1191.81, 1164.32, 1101.17, 1056.82, 1035.60, 1014.39, 927.61, 912.18, 835.11, 742.47, 719.33, 694.26, 647.98 cm⁻¹; ¹H NMR (400 MHz, CDCl₃): δ 7.62 (s, 1H, 13-CH), 7.42 (t, *J* = 6.8 Hz, 2H, Ar-H), 7.13 (t, *J* = 8.8 Hz, 2H, Ar-H), 5.29 (d, *J* = 10.4 Hz, 1H, 1-CH), 3.96 (t, *J* = 8 Hz, 1H, 6-CH), 3.27 (t, *J* = 3.8 Hz, 1H, 5-CH), 2.83 (d, *J* = 8.8 Hz, 1H, 7-CH), 2.44–2.41 (m, 1H, 9-CH), 2.25–2.08 (m, 4H, 2-CH₂, 9-CH, 3-CH), 1.47–1.41 (m, 1H, 8-CH), 1.65 (s, 3H, 14-CH₃), 1.31–1.25 (m, 5H, 15-CH₃, 3-CH, 8-CH) ppm; ¹³C NMR (100 MHz, CDCl₃): δ 170.7, 164.3, 161.8, 136.9, 134.6, 131.8, 129.7, 128.8, 125.1, 115.9, 82.9, 66.4, 61.6, 46.7, 41.8, 36.0, 29.9, 23.2, 17.4 ppm. HRMS calcd for C₂₁H₂₄FO₃, (M+H)⁺: 343.1709 Found 343.1715.

5.1.4. Synthesis of (E)-13-(3-thiopheno)parthenolide (5f)—White solid; mp: 183–185 °C; IR: 3353.61, 2915.89, 2850.32, 1720.22, 1608.37, 1591.01, 1515.80, 1436.41, 1380.80, 1299.81, 1267.02, 1193.24, 1162.81, 1064.53, 1000.89, 914.04, 873.61, 823.47, 806.11, 746.3, 674.97, 638.33 cm⁻¹; ¹H NMR (400 MHz, CDCl₃): δ 7.65 (d, *J* = 2.8 Hz, 1H, 13-CH), 7.51 (s, 1H, 3'-CH), 7.41 (s, 1H, 4'-CH), 7.20 (d, *J* = 4.4 Hz, 1H, 2'-CH), 5.29 (d, *J* = 12 Hz, 1H, 1-CH), 3.98 (t, *J* = 6.8 Hz, 1H, 6-CH), 3.18 (m, 1H, 5-CH), 2.83 (d, *J* = 8.8 Hz, 1H, 7-CH), 2.43 (m, 1H, 9-CH), 2.16–2.30 (m, 5H, 2-CH₂, 9-CH, 3-CH, 8-CH), 1.72 (s, 3H, 14-CH₃), 1.54 (m, 1H, 3-CH), 1.33 (s, 3H, 15-CH₃), 1.26–1.31 (m, 1H, 8-CH) ppm; ¹³C NMR (100 MHz, CDCl₃): δ 171.09, 135.37, 134.52, 131.85, 129.28, 127.78, 127.33, 126.49, 125.42, 82.7, 66.41, 61.64, 46.92, 42.10, 35.99, 30.56, 24.36, 17.52, 17.30 ppm. HRMS calcd for C₁₉H₂₃O₃S (M+H)⁺: 331.1368 Found 331.1356.

5.1.5. Synthesis of (E)-13-(2-thiophenyl)parthenolide (5g)—White solid; mp: 64–66 °C; IR: 2913.96, 2850.32, 1735.65, 1627.65, 1417.45, 1380.80, 1342.23, 1236.17, 1184.10, 1137.81, 1120.46, 1024.03, 1006.86, 979.68, 912.18, 829.25, 800.33, 705.83, 663.43, 628.69 cm⁻¹; ¹H NMR (400 MHz, CDCl₃): δ 7.80 (s, 1H, 13-CH), 7.58 (d, *J* = 5.6

Hz, 1H, 4'-CH), 7.32 (d, $J = 5.1$ Hz, 1H, 2'-CH), 7.16 (t, $J = 3.2$ Hz, 1H, 3'-CH), 5.33 (d, $J = 11.0$ Hz, 1H, 1-CH), 4.06 (t, $J = 8.0$ Hz, 1H, 6-CH), 3.86 (t, $J = 3.2$ Hz, 1H, 5-CH), 2.82 (d, $J = 9.2$ Hz, 1H, 7-CH), 2.47–2.39 (m, 2H, 2-CH, 9-CH), 2.17–2.22 (m, 1H, 2-CH), 2.07–1.81 (m, 2H, 9-CH, 3-CH), 1.69 (s, 3H, 14-CH₃), 1.59–1.57 (m, 1H, 8-CH), 1.32–1.26 (m, 5H, 15-CH₃, 3-CH, 8-CH) ppm. ¹³C NMR (CDCl₃, 100 MHz): δ 171.26, 137.05, 134.89, 133.50, 130.97, 130.90, 128.30, 125.79, 121.46, 83.03, 66.49, 61.96, 47.04, 42.51, 36.10, 31.36, 24.68, 17.83, 17.65 ppm. HRMS calcd for C₁₉H₂₃O₃S (M+H)⁺: 331.1368 Found 331.1358.

5.1.6. Synthesis of (E)-13-(pyrimidinyl)parthenolide (5h)—White solid; mp: 207–209 °C; IR: 3031.60, 2931.32, 1749.15, 1660.44, 1648.87, 1591.01, 1552.44, 1517.73, 1411.66, 1349.95, 1332.59, 1249.67, 1232.31, 1209.24, 1191.81, 1164.32, 1101.17, 1056.82, 1035.60, 1014.39, 927.61, 912.18, 835.11, 742.47, 719.33, 694.26, 647.98 cm⁻¹; ¹H NMR (400 MHz, CDCl₃): δ 9.2 (s, 1H, 2'-CH), 8.83 (s, 2H, 4'-CH, 6'-CH), 7.56 (d, $J = 3.2$ Hz, 1H, 13-CH), 5.28 (d, $J = 10.8$ Hz, 1H, 1-CH), 4.00 (t, $J = 8.8$ Hz, 1H, 6-CH), 3.3 (m, 1H, 5-CH), 2.83 (d, $J = 9.2$ Hz, 1H, 7-CH), 2.44–2.41 (m, 1H, 9-CH), 2.22–2.01 (m, 5H, 2-CH₂, 9-CH, 3-CH, 8-CH), 1.69 (s, 3H, 14-CH₃), 1.32–1.26 (m, 5H, 15-CH₃, 3-CH, 8-CH) ppm; ¹³C NMR (CDCl₃, 100 MHz): δ 169.7, 158.7, 157.2, 155.09, 134.5, 130.4, 128.2, 125.7, 83.3, 66.5, 47.02, 41.8, 36.2, 31.1, 31.8, 30.4, 24.5, 17.7, 17.5 ppm. HRMS calcd for C₁₉H₂₃N₂O₃, (M+H)⁺: 32.11709 Found 327.1717.

5.2.0. General synthetic procedure for the allylic oxidation of parthenolide analogs 5a–5h and 7

The aryl substituted parthenolide analogs **5a–5h** (1 mmol) individually was treated with selenium dioxide (0.5 mmol) in the presence of *tert*-butyl hydrogen peroxide (3.8 mmol) in dichloromethane at room temperature overnight. Then, 5 ml of water was added to the reaction and the resulting mixture extracted with dichloromethane (2 × 20 ml). The combined organic layers were separated, dried over anhydrous Na₂SO₄, filtered, concentrated, and purified by flash column chromatography to furnish the corresponding 13-aryl substituted MMB analogues **6a–6h** and **8** (20–30 mg) in 50 to 60% yield.

5.2.1. Synthesis of (E)-13-(phenyl)MMB (6a)

White solid; mp: 115–117 °C; IR: 3530.42, 2965.23, 2936.52, 1763.45, 1675.26, 1487.49, 1444.15, 1398.74, 1269.51, 1242.67, 1200.08, 1190.26, 1125.66, 1094.58, 1043.28, 1012.43, 988.56, 955.21, 925.1, 902.13, 852.42, 812.12, 809.21, 7555.35, 746.98 cm⁻¹; ¹H NMR (400 MHz, CDCl₃): δ 7.73 (d, $J = 2.8$ Hz, 1H, 13-CH), 7.43–7.35 (m, 5H, Ar-H), 5.65 (t, $J = 7.6$ Hz, 1H, 1-CH), 4.13–4.07 (m, 2H, 14-CH₂), 3.86 (t, $J = 8.4$ Hz, 1H, OH), 3.28 (t, $J = 8.4$ Hz, 1H, 6-CH), 2.91 (d, $J = 8.8$ Hz, 1H, 5-CH), 2.34–2.10 (m, 6H, 2-CH₂, 3-CH₂, 8-CH₂), 1.52 (s, 3H, 15-CH₃), 1.05–1.21 (m, 3H, 7-CH, 9-CH₂) ppm; ¹³C NMR (100 MHz, CDCl₃): δ 171.01, 139.7, 138.9, 134.2, 132.7, 129.7, 129.3, 128.7, 128.4, 127.2, 80.5, 65.7, 63.06, 60.5, 60.4, 42.7, 36.5, 24.5, 24.4, 23.6, 18.1 ppm. HRMS calcd for C₂₁H₂₅O₄ (M+H)⁺: 341.1753 Found 341.1758.

5.2.2. Synthesis of (E)-13-(4-aminophenyl)MMB (6b)

Light yellow solid; mp: 179–181 °C; IR: 3448.15, 3355.59, 2962.17, 1737.58, 1645.01, 1627.65, 1591.01, 1569.81, 1490.73, 1429.02, 1417.45, 1382.66, 1321.62, 1303.66, 1286.3, 1272.81, 1240.02, 1186.21, 1137.81, 1089.61, 1045.25, 1000.89, 981.61, 910.25, 829.25, 748.26, 700.97, 634.51 cm^{-1} ; ^1H NMR (CDCl_3 , 400 MHz): δ 7.64 (d, $J = 2.8$ Hz, 1H, 13-CH), 7.24 (d, $J = 8.4$ Hz, 2H, Ar-H), 6.17 (d, $J = 8$ Hz, 2H, Ar-H), 5.68 (t, $J = 7.2$ Hz, 1H, 1-CH), 4.30-4.25 (m, 1H, 14-CH), 4.19-4.16 (m, 1H, 14-CH), 3.95 (s, 2H, NH_2), 3.89 (t, $J = 9.2$ Hz, 1H, 6-CH), 3.27 (t, $J = 3.2$ Hz, 1H, OH), 2.95 (d, $J = 2.8$ Hz, 1H, 5-CH), 2.70 (t, $J = 3.0$ Hz, 1H, 7-CH), 2.31-2.15 (m, 4H, 2 CH_2 , 9- CH_2), 1.56 (s, 3H, 15- CH_3), 1.38 (d, $J = 5.6$ Hz, 1H, 8-CH), 1.25 (s, 2H, 3- CH_2), 1.11 (t, $J = 10.4$ Hz, 1H, 8-CH) *ppm*. ^{13}C NMR (100 MHz, CDCl_3): δ 171.90, 148.04, 140.11, 139.77, 133.44, 131.36, 127.40, 125.63, 123.90, 114.51, 80.45, 66.23, 63.27, 60.63, 43.06, 36.67, 29.84, 24.61, 23.83, 18.38 *ppm*. HRMS calcd for $\text{C}_{21}\text{H}_{26}\text{NO}_4$ ($\text{M}+\text{H}$) $^+$: 356.1862 Found 356.1857.

5.2.3. Synthesis of (E)-13-(2-bromophenyl)MMB (6c)

White solid; mp: 185–187 °C; IR: 3525.29, 2956.4, 2925.32, 1743.36, 1643.08, 1463.73, 1430.95, 1390.45, 1245.81, 1222.67, 1189.88, 1170.6, 1116.46, 1072.24, 1031.75, 1000.89, 981.61, 941.82, 939.1, 898.68, 850.47, 817.68, 800.33, 754.04, 736.69, 671.12, 632.55 cm^{-1} ; ^1H NMR (400 MHz, CDCl_3): δ 7.69-7.40 (m, 2H, 13-CH, 3'-CH), 7.41-7.26 (m, 3H, Ar-H), 5.64 (t, $J = 3.2$ Hz 1H, 1-CH), 4.02 (s, 2H, 14- CH_2), 3.92 (t, $J = 9.2$ Hz, 1H, 6-H), 3.18 (t, $J = 3.2$ Hz, 1H, OH), 2.90 (d, $J = 8.8$ Hz, 1H, 5-CH), 2.23-2.01 (m, 5H, 7-CH, 2- CH_2 , 9- CH_2), 1.54 (s, 3H, 15- CH_3), 1.33-1.25 (m, 3H, 3- CH_2 , 8-CH), 1.09 (t, $J = 10.8$ Hz, 1H, 8-CH) *ppm*; ^{13}C NMR (100 MHz, CDCl_3): δ 170.4, 139.7, 137.7, 135.4, 133.0, 131.7, 130.7, 129.5, 127.3, 127.2, 123.6, 80.6, 65.7, 63.2, 60.6, 43.0, 36.7, 24.7, 24.4, 23.7, 18.2 *ppm*. HRMS calcd for $\text{C}_{21}\text{H}_{24}\text{BrO}_4$ ($\text{M}+\text{H}$) $^+$: 419.0858 Found 419.0861.

5.2.4. Synthesis of (E)-13-(4-fluorophenyl)MMB (6d)

oily mass, IR: 3472.42; 2935, 2912.13, 1725.25, 1669.15, 1625.46, 1589.26, 1565.89, 1503.94, 1463.66, 1379.09, 1343.65, 1232.55, 1232.56, 1211.23, 1178.87, 1165.32, 1123.34, 1043.48, 1045.20, 1027.45, 956.87, 932.48, 887.87, 756.47, 728.29, 692.22, 654.12 cm^{-1} ; ^1H NMR (400 MHz, CDCl_3): δ 7.68 (d, $J = 2.8$ Hz, 1H, 13-CH), 7.42-7.38 (m, 2H, Ar-H), 7.13 (t, $J = 8.8$ Hz, 2H, Ar-H), 5.64 (t, $J = 3.2$ Hz, 1H, 1-CH), 4.16-4.12 (m, 2H, 14- CH_2), 3.88 (t, $J = 9.2$ Hz, 1H, 6-CH), 3.37 (brs, 1H, OH), 2.94 (d, $J = 9.2$ Hz, 1H, 5H), 2.42 (t, $J = 3.0$ Hz, 1H, 7-CH), 2.23-2.14 (m, 4H, 2 CH_2 , 9- CH_2), 1.54 (s, 3H, 15- CH_3), 1.27-1.25 (m, 3H, 3- CH_2 , 8-CH), 1.11 (t, $J = 9.6$ Hz, 1H, 8-CH) *ppm*; ^{13}C NMR (100 MHz, CDCl_3): δ 171.25, 164.52 and 162.03 (C-F), 139.93, 137.95, 131.19, 130.32, 127.81, 115.79, 80.6, 66.15, 63.24, 63.21, 60.79, 42.99, 36.71, 29.93, 24.68, 23.86, 18.39 *ppm*. HRMS calcd for $\text{C}_{21}\text{H}_{24}\text{FO}_4$ ($\text{M}+\text{H}$) $^+$: 359.1659 Found 359.1666.

5.2.5. Synthesis of (E)-13-(3-trifluoromethylphenyl)MMB (6e)

White solid; mp: 152–154 °C; IR: 3432.73, 2912.03, 2846.46, 1726.01, 1625.72, 1436.32, 1415.64, 1382.41, 1322.91, 1286.31, 1236.17, 1176.38, 1168.67, 1116.67, 1037.53, 1010.53, 997.03, 894.82, 850.42, 811.90, 698.12, 617.12 cm^{-1} ; ^1H NMR (400 MHz, CDCl_3): δ 7.73 (d, $J = 2.8$ Hz, 1H, 13-CH), 7.65 (d, $J = 8.4$ Hz, 2H, Ar-H), 7.60 (d, $J = 8.4$

Hz, 2H, Ar-H), 5.69 (t, $J = 7.6$ Hz, 1H, 1-CH), 4.11-4.09 (m, 2H, 14-CH₂), 3.90 (t, $J = 8.4$ Hz, 1H, 6-CH), 3.39 (brs, 1H, OH), 2.96 (d, $J = 9.6$ Hz, 1H, 5-CH), 2.27-2.13 (m, 5H, 7-CH, 2-CH₂, 9-CH₂), 1.55 (s, 3H, 15-CH₃), 1.26 (m, 3H, 3-CH₂, 8-CH), 1.11 (t, $J = 9.8$ Hz, 1H, 8-CH) ppm; ¹³C NMR (100 MHz, CDCl₃): δ 170.61, 139.24, 136.86, 136.80, 135.06, 132.17, 131.65, 129.14, 127.86, 125.91, 125.33, 80.55, 65.75, 62.88, 60.59, 42.86, 36.45, 31.59, 24.77, 23.62, 22.66, 18.14 ppm. HRMS calcd for C₂₂H₂₄F₃O₄ (M+H)⁺: 409.1627 Found 409.1622.

5.2.6. Synthesis of (E)-13-(3-thiophenyl)MMB (6f)

White solid; mp: 207–209 °C; IR: 3488.65, 2948.12, 2912.6, 1737.58, 1633.44, 1450.23, 1430.95, 1380.81, 1334.23, 1263.17, 1211.10, 1193.74, 1164.81, 1120.46, 1068.39, 1049.10, 1029.82, 1004.75, 921.82, 898.68, 865.90, 811.90, 809.97, 796.47, 744.40, 701.97, 624.83 cm⁻¹; ¹H NMR (400 MHz, CDCl₃): δ 7.65 (s, 1H, 13-CH), 7.50 (s, 1H, 2'-CH), 7.40 (s, 1H, 5'-CH), 7.11 (s, 1H, 4'-CH), 5.68 (t, $J = 3.2$ Hz, 1H, 1-H), 4.25-4.11 (m, 2H, 14-CH₂), 3.88 (t, $J = 8.4$ Hz, 1H, 6-CH), 3.29 (brs, 1H, OH), 2.95 (d, $J = 9.6$ Hz, 1H, 5-CH), 2.66 (t, $J = 3.2$ Hz, 1H, 7-CH), 2.27-2.13 (m, 5H, 2-CH₂, 9-CH₂, 3-CH), 1.55 (s, 3H, 15-CH₃), 1.26 (m, 2H, 3-CH, 8-CH), 1.11 (t, $J = 11.6$ Hz, 1H, 8-CH) ppm; ¹³C NMR (100 MHz, CDCl₃): δ 171.3, 139.9, 135.3, 133.1, 133.1, 128.9, 128.0, 127.3, 126.4, 80.5, 66.3, 63.1, 60.6, 43.0, 36.6, 24.9, 24.6, 23.8, 18.3 ppm. HRMS calcd for C₁₉H₂₃O₄S (M+H)⁺: 347.1317 Found 347.1323.

5.2.7. Synthesis of (E)-13-(2-thiophenyl)MMB (6g)

White solid; mp: 103–105 °C; IR: 3432.73, 2912.03, 2846.46, 1726.01, 1625.72, 1436.32, 1415.64, 1382.41, 1322.91, 1286.31, 1236.17, 1176.38, 1168.67, 1116.67, 1037.53, 1010.53, 997.03, 894.82, 850.42, 811.90, 698.12, 617.12 cm⁻¹; ¹H NMR (CDCl₃, 400 MHz): δ 7.8 (d, $J = 6.2$ Hz, 1H, 13-CH), 7.54 (d, $J = 5.2$ Hz, 1H, 3'-CH), 7.32 (d, $J = 5.2$ Hz, 1H, 5'-CH), 7.13 (t, $J = 4.0$ Hz, 1H, 4'-CH), 5.70 (t, $J = 8.0$ Hz, 1H, 1-CH), 4.44 (dd, $J = 6.4, 12.4$ Hz, 1H, 14-CH), 4.24 (dd, $J = 3.6, 12.8$ Hz, 1H, 14-CH), 3.92 (t, $J = 8.4$ Hz, 1H, 6-CH), 3.21 (t, $J = 3.0$ Hz, 1H, OH), 3.11-3.08 (m, 1H, 5-CH), 2.94 (d, $J = 9.2$ Hz, 1H, 7-CH), 2.33-2.14 (m, 4H, 2-CH₂, 9-CH₂), 1.59 (s, 3H, 15-CH₃), 1.48-1.43 (m, 2H, 3-CH₂), 1.27-1.24 (m, 1H, 8-CH), 1.11 (t, $J = 9.7$ Hz, 1H, 8-CH) ppm; ¹³C NMR (CDCl₃, 100 MHz): δ 171.52, 139.95, 136.40, 132.89, 131.64, 131.53, 130.18, 127.76, 127.04, 80.47, 66.56, 63.17, 60.80, 43.02, 36.65, 24.64, 24.55, 23.95, 18.49 ppm; HRMS calcd for C₁₉H₂₃O₄S (M+H)⁺: 347.1317 Found 347.1311.

5.2.8. Synthesis of (E)-13-(pyrimidinyl) MMB (6h)

White solid; mp: 214–216 °C; IR: 3485.23, 3045.21, 2943.24, 1745.46, 1674.24, 1656.45, 1584.27, 1565.78, 1525.78, 1415.54, 1357.35, 1345.25, 1245.58, 1226.89, 1212.28, 1196.87, 1174.23, 1110.56, 1045.22, 1046.56, 1021.13, 934.51, 914.16, 838.16, 745.86, 726.28, 691.03, 635.09 cm⁻¹; ¹H NMR (CDCl₃, 400 MHz): δ 9.22 (s, 1H, 13-CH), 8.87 (s, 2H, 4'-CH, 6'-CH), 7.60 (d, $J = 3.2$ Hz, 1H, 2'-CH), 5.29 (t, $J = 7.2$ Hz, 1H, 1-CH), 4.21 (d, $J = 12.0$ Hz, 1H, 14-CH), 4.13 (d, $J = 12.0$ Hz, 1H, 14-CH), 3.94 (t, $J = 8.8$ Hz, 1H, 6-CH), 3.58 (t, $J = 3.0$ Hz, 1H, OH), 2.97 (d, $J = 9.6$ Hz, 1H, 5-CH), 2.18-2.21 (m, 3H, 7-CH, 9-CH₂), 1.56 (m, 4H, 15-CH₃, 2-CH), 1.26-1.33 (m, 3H, 3-CH₂, 2-CH), 1.14-1.03 (m, 2H, 8-

CH₂)*ppm*; ¹³C NMR (CDCl₃, 100 MHz): δ 170.04, 158.5, 156.7, 139.1, 134.8, 130.5, 129.2, 80.7, 66.6, 62.9, 60.8, 43.4, 36.6, 29.9, 25.5, 25.3, 23.8, 18.3 *ppm*; HRMS calcd for C₁₉H₂₃N₂O₄ (M+H)⁺: 343.1658 Found 343.1662.

5.3.0. Synthesis of parthenolide Michael adduct 7

13-(2-Iodoimidazole) Michael adducts **7** was synthesized utilizing the reported literature procedures [23].

5.3.1. 13-(2-iodoimidazole)parthenolide Michael adduct (7)

mp: 199–200 °C; IR: 2946.58, 2859.89, 1758.32, 1673.56, 1456.24, 1333.45, 1278.87, 1232.54, 1194.76, 1171.32, 1133.57, 1087.54, 1067.26, 1020.23, 984.62, 923.78, 872.97, 846.54, 818.15, 745.17, 645.15, 617.19 cm⁻¹; ¹H NMR (400 MHz, DMSO-d₆): δ 7.34 (s, 1H, 4'-CH), 6.99 (s, 1H, 5'-CH), 5.12 (d, *J* = 10.0 Hz, 1H, 1-CH), 4.34–4.07 (m, 2H, 13-CH₂), 4.05 (t, *J* = 9.2 Hz, 1H, 6-CH), 3.04–2.99 (m, 1H, 5-CH), 2.70 (d, *J* = 8.8 Hz, 1H, 7-CH), 2.34–2.30 (m, 1H, 2-CH), 2.14–1.98 (m, 5H, 9-CH₂, 2-CH, 3-CH, 8-CH), 1.59 (s, 3H, 14-CH₃), 1.30 (d, *J* = 15.6 Hz, 1H, 11-CH), 1.11–1.05 (m, 5H, 15-CH₃, 3-CH, 8-CH) *ppm*; ¹³C NMR (100 MHz, DMSO-d₆): δ 174.9, 134.2, 131.9, 124.4, 124.1, 119.4, 81.5, 65.1, 61.1, 47.2, 46.1, 40.3, 38.7, 35.8, 28.7, 23.5, 16.7, 16.5 *ppm*. HRMS calcd for C₁₈H₂₄IN₂O₃ (M+H)⁺: 443.0832 Found 443.0839.

5.3.2. 13-(2-iodoimidazole)MMB (8)

White solid; mp: 206–208 °C; IR: 3492.51, 2913.96, 2871.53, 1749.15, 1662.37, 1429.02, 1326.51, 1272.82, 1224.60, 1191.81, 1160.96, 1124.31, 1099.24, 1081.99, 1014.39, 995.10, 914.11, 863.97, 829.25, 806.11, 728.97, 655.69, 615.19 cm⁻¹; ¹H NMR (CDCl₃, 400 MHz): δ 7.22 (s, 1H, 4'-CH), 7.15 (s, 1H, 5'-CH), 5.59 (t, *J* = 7.6 Hz, 1H, 1-CH), 4.35 (dd, *J* = 8.8, 14.8 Hz, 2H, 14-CH₂), 3.87–3.94 (m, 3H, 6-CH, OH, 5-CH), 2.74–2.78 (m, 2H, 13-CH₂), 2.08–2.35 (m, 7H, 9-CH₂, 2-CH₂, 3-CH, 11-CH, 7-CH), 1.63–1.54 (m, 5H, 3-CH, 8-CH, 15-CH₃), 1.05 (t, 1H, *J* = 9.6 Hz, 8-CH) *ppm*. ¹³C NMR (CDCl₃, 100 MHz): δ 176.40, 141.43, 132.43, 125.43, 124.85, 81.15, 64.69, 63.39, 61.0, 48.22, 47.06, 43.48, 37.65, 26.53, 25.22, 23.80, 18.35 *ppm*; HRMS calcd for C₁₈H₂₄IN₂O₄ (M+H)⁺: 459.0781 Found 459.0775.

5.4. Biological Assays

5.4.0. Oocyte culture—Immature stage VI *Xenopus* oocytes were isolated and cultured as described previously [35]. For assays of bioactivity, compounds were dissolved in DMSO, added to culture media at a final concentration of 100 μM, and incubated overnight. For each compound treatment, 20 oocytes were used per well of a multiwell tissue culture plate. The next morning, oocyte maturation was assessed by determining if a white spot had formed at the oocyte animal poles. A white spot is a morphological indicator that germinal vesicle (nuclear) breakdown (GVBD) has occurred, as the upward migration of the nucleus during GVBD displaces the dark animal hemisphere pigment at the animal pole. Oocytes treated with compounds that did not induce maturation overnight, were subsequently stimulated with 2 μg/ml progesterone [36] and the rate to GVBD was scored relative to DMSO-only treated controls. Where indicated, oocytes were harvested when 50% of the DMSO oocytes reached GVBD and segregated into those that had not (-) or had (+) completed GVBD.

Animal protocols were approved by the UAMS Institutional Animal Care and Use committee, in accordance with Federal regulations.

5.4.1. Western blot analyses—Oocytes were lysed in NP40 lysis buffer containing sodium vanadate and a protease inhibitor cocktail (Sigma) as previously described [37]. Briefly, the lysate was spun, clarified and transferred immediately to 1X LDS sample buffer (Nupage). The lysates were run on a 10% Nupage gel and transferred to a 0.2 μ m-pore-size nitrocellulose filter (Protran; Midwest Scientific). The membrane was blocked with 1% bovine serum albumin (Sigma) for 60 min at room temperature. The phospho-specific Cdc2 antibody (Cell Signaling) was used at 1:1000 and detects the inhibitory Tyr15 phosphorylation. The phospho-specific MAP kinase antibody (Cell Signaling) was used at 1:1000 and detects the activating phosphorylations at both Thr202 and Tyr204. Sigma antibodies to Tubulin were used at 1:20,000. The filters were visualized with horseradish peroxidase conjugated anti-Rabbit antibody using enhanced chemiluminescence in a Fluorchem 8000 Advanced Imager (Alpha Innotech Corp.).

Supplementary Material

Refer to Web version on PubMed Central for supplementary material.

Acknowledgments

We are grateful to NCI/NIH grant R01 CA158275 (to P.A.C); the Arkansas Research Alliance (ARA) for financial support (to PAC); NIH grant RO1 HD35688, a Sturgis Diabetes Research Pilot Award, an Arkansas Breast Cancer Research Program award, the UAMS College of Medicine Research Council, and support from a NIGMS IDeA program award P30 GM110702 (to AMM); a UAMS Translational Research Institute award supported by the NIH National Center for Research Resources grants UL1 TR0000039 and KL2TR000063 (to A.M.M. and P.A.C); and the NCI Developmental Therapeutic Program (DTP) for screening data. We are also grateful to the Mass Spectrometry Facility, Chemistry Department, University of California, Riverside, for accurate mass data (NSF grant CHE-0541848) and to Dr. Darin Jones, University of Arkansas, Little Rock, for access to IR spectroscopic facilities.

References and notes

1. Heptinstall S, Groenewegen WA, Spangenberg P, Losche W. Inhibition of platelet behaviour by feverfew: a mechanism of action involving sulphhydryl groups. *Folia Haematol Int Mag Klin Morphol Blutforsch.* 1988; 115:447–449. [PubMed: 2465950]
2. Hall IH, Lee KH, Starnes CO, Sumida Y, Wu RY, Waddell TG, Cochran JW, Gerhart KG. Anti-inflammatory activity of sesquiterpene lactones and related compounds. *J Pharm Sci.* 1979; 68:537–542. [PubMed: 311831]
3. Pfaffenrath V, Diener HC, Fischer M, Friede M, Henneicke-von Zepelin HH. Investigators The efficacy safety of Tanacetum parthenium (feverfew) in migraine prophylaxis--a double-blind, multicentre, randomized placebo-controlled dose-response study. *Cephalalgia.* 2002; 22:523–532. [PubMed: 12230594]
4. Sun Y, St Clair DK, Fang F, Warren GW, Rangnekar VM, Crooks PA, St Clair WH. The radiosensitization effect of parthenolide in prostate cancer cells is mediated by nuclear factor- κ B inhibition and enhanced by the presence of PTEN. *Mol Cancer Ther.* 2007; 6:2477–2486. [PubMed: 17876045]
5. Wen J, You KR, Lee SY, Song CH, Kim DG. Oxidative stress-mediated apoptosis. The anticancer effect of the sesquiterpene lactone parthenolide. *J Biol Chem.* 2002; 277:38954–38964. [PubMed: 12151389]

6. Patel NM, Nozaki S, Shortle NH, Bhat-Nakshatri P, Newton TR, Rice S, Gelfanov V, Boswell SH, Goulet RJ Jr, Sledge GW Jr, Nakshatri H. Paclitaxel sensitivity of breast cancer cells with constitutively active NF- κ B is enhanced by IkappaBalpha super-repressor and parthenolide. *Oncogene*. 2000; 19:4159–4169. [PubMed: 10962577]
7. Mendonca MS, Hardacre M, Datzman N, Comerford K, Chin-Sinex H, Sweeney C. Inhibition of constitutive NF κ B activity by the anti-inflammatory sesquiterpene, parthenolide slows cell growth and increases radiation sensitivity. *International Journal of Radiation Oncology*Biophysics*. 2003; 57:S354.
8. Marin GH, Mansilla E. Apoptosis induced by Magnolia Grandi flora extract in chlorambucil-resistant B-chronic lymphocytic leukemia cells. *J Cancer Res Ther*. 2010; 6:463–465. [PubMed: 21358081]
9. Lopez-Franco O, Hernandez-Vargas P, Ortiz-Munoz G, Sanjuan G, Suzuki Y, Ortega L, Blanco J, Egido J, Gomez-Guerrero C. Parthenolide modulates the NF- κ B-mediated inflammatory responses in experimental atherosclerosis. *Arterioscler Thromb Vasc Biol*. 2006; 26:1864–1870. [PubMed: 16741149]
10. Ralstin MC, Gage EA, Yip-Schneider MT, Klein PJ, Wiebke EA, Schmidt CM. Parthenolide cooperates with NS398 to inhibit growth of human hepatocellular carcinoma cells through effects on apoptosis and G0-G1 cell cycle arrest. *Mol Cancer Res*. 2006; 4:387–399. [PubMed: 16778086]
11. Won YK, Ong CN, Shen HM. Parthenolide sensitizes ultraviolet (UV)-B-induced apoptosis via protein kinase C-dependent pathways. *Carcinogenesis*. 2005; 26:2149–2156. [PubMed: 16051639]
12. Oka D, Nishimura K, Shiba M, Nakai Y, Arai Y, Nakayama M, Takayama H, Inoue H, Okuyama A, Nonomura N. Sesquiterpene lactone parthenolide suppresses tumor growth in a xenograft model of renal cell carcinoma by inhibiting the activation of NF- κ B. *Int J Cancer*. 2007; 120:2576–2581. [PubMed: 17290398]
13. Kupchan SM, Eakin MA, Thomas AM. Tumor inhibitors. 69. Structure-cytotoxicity relationships among the sesquiterpene lactones. *J Med Chem*. 1971; 14:1147–1152. [PubMed: 5116225]
14. Rodriguez ET, ; Mitchell GHN, C J. Biological activities of sesquiterpene lactones. *Phytochemistry*. 1976; 15:1573–1580.
15. Hehner SP, Heinrich M, Bork PM, Vogt M, Ratter F, Lehmann V, Schulze-Osthoff K, Droge W, Schmitz ML. Sesquiterpene lactones specifically inhibit activation of NF- κ B by preventing the degradation of I kappa B-alpha and I kappa B-beta. *J Biol Chem*. 1998; 273:1288–1297. [PubMed: 9430659]
16. Kupchan SM, Fessler DC, Eakin MA, Giacobbe TJ. Reactions of alpha methylene lactone tumor inhibitors with model biological nucleophiles. *Science*. 1970; 168:376–378. [PubMed: 5435896]
17. Hanson RL, Lardy HA, Kupchan SM. Inhibition of phosphofructokinase by quinone methide and alpha-methylene lactone tumor inhibitors. *Science*. 1970; 168:378–380. [PubMed: 4244949]
18. Gopal YN, Arora TS, Van Dyke MW. Parthenolide specifically depletes histone deacetylase 1 protein and induces cell death through ataxia telangiectasia mutated. *Chem Biol*. 2007; 14:813–823. [PubMed: 17656318]
19. Kim YJ, Choi MH, Hong ST, Bae YM. Resistance of cholangiocarcinoma cells to parthenolide-induced apoptosis by the excretory-secretory products of *Clonorchis sinensis*. *Parasitol Res*. 2009; 104:1011–1016. [PubMed: 19066964]
20. Riganti C, Doublier S, Viariso D, Miraglia E, Pescarmona G, Ghigo D, Bosia A. Artemisinin induces doxorubicin resistance in human colon cancer cells via calcium-dependent activation of HIF-1alpha and P-glycoprotein overexpression. *Br J Pharmacol*. 2009; 156:1054–1066. [PubMed: 19298255]
21. Dell'Agli M, Galli GV, Bosisio E, D'Ambrosio M. Inhibition of NF- κ B and metalloproteinase-9 expression and secretion by parthenolide derivatives. *Bioorg Med Chem Lett*. 2009; 19:1858–1860. [PubMed: 19269818]
22. Sweeney CJ, Mehrotra S, Sadaria MR, Kumar S, Shortle NH, Roman Y, Sheridan C, Campbell RA, Murry DJ, Badve S, Nakshatri H. The sesquiterpene lactone parthenolide in combination with docetaxel reduces metastasis and improves survival in a xenograft model of breast cancer. *Mol Cancer Ther*. 2005; 4:1004–1012. [PubMed: 15956258]

23. Neelakantan S, Nasim S, Guzman ML, Jordan CT, Crooks PA. Aminoparthenolides as novel anti-leukemic agents: Discovery of the NF-kappaB inhibitor, DMAPT (LC-1). *Bioorg Med Chem Lett.* 2009; 19:4346–4349. [PubMed: 19505822]
24. Guzman ML, Jordan CT. Feverfew: weeding out the root of leukaemia. *Expert Opin Biol Ther.* 2005; 5:1147–1152. [PubMed: 16120045]
25. Guzman ML, Rossi RM, Karnischky L, Li X, Peterson DR, Howard DS, Jordan CT. The sesquiterpene lactone parthenolide induces apoptosis of human acute myelogenous leukemia stem and progenitor cells. *Blood.* 2005; 105:4163–4169. [PubMed: 15687234]
26. Nasim S, Crooks PA. Antileukemic activity of aminoparthenolide analogs. *Bioorg Med Chem Lett.* 2008; 18:3870–3873. [PubMed: 18590961]
27. Hwang DR, Wu YS, Chang CW, Lien TW, Chen WC, Tan UK, Hsu JT, Hsieh HP. Synthesis and anti-viral activity of a series of sesquiterpene lactones and analogues in the subgenomic HCV replicon system. *Bioorg Med Chem.* 2006; 14:83–91. [PubMed: 16140536]
28. Nasim S, Pei S, Hagen FK, Jordan CT, Crooks PA. Melampomagnolide B: a new antileukemic sesquiterpene. *Bioorg Med Chem.* 2011; 19:1515–1519. [PubMed: 21273084]
29. Han C, Barrios FJ, Rioski MV, Colby DA. Semisynthetic derivatives of sesquiterpene lactones by palladium-catalyzed arylation of the alpha-methylene-gamma-lactone substructure. *J Org Chem.* 2009; 74:7176–7179. [PubMed: 19697954]
30. Penthala NR, Janganati V, Parkin S, Varughese KI, Crooks PA. (E)-13-(4-Amino-phen-yl)parthenolide. *Acta Crystallogr Sect E Struct Rep Online.* 2013; 69:o1709–o1710.
31. Lasko P. Translational control during early development. *Progress in molecular biology and translational science.* 2009; 90:211–254. [PubMed: 20374743]
32. Wickens, M.; Goodwin, EB.; Kimble, J.; Strickland, S.; Hentze, MW. Translational Control of Developmental Decisions. In: Sonenberg, N.; Hershey, J.; Mathews, MB., editors. *Translational Control of Gene Expression.* Cold Spring Harbor Laboratory Press; 2000. p. 295-370.
33. MacNicol MC, MacNicol AM. Developmental timing of mRNA translation - integration of distinct regulatory elements. *Mol Reprod Dev.* 2010; 77:662–669. [PubMed: 20652998]
34. Janganati V, Penthala NR, Cragle CE, Macnicol AM, Crooks PA. Heterocyclic aminoparthenolide derivatives modulate G2-M cell cycle progression during *Xenopus* oocyte maturation. *Bioorg Med Chem Lett.* 2014; 24:1963–1967. [PubMed: 24656611]
35. Machaca K, Haun S. Induction of maturation-promoting factor during *Xenopus* oocyte maturation uncouples Ca(2+) store depletion from store-operated Ca(2+) entry. *J Cell Biol.* 2002; 156:75–85. [PubMed: 11781335]
36. Howard EL, Charlesworth A, Welk J, MacNicol AM. The mitogen-activated protein kinase signaling pathway stimulates mos mRNA cytoplasmic polyadenylation during *Xenopus* oocyte maturation. *Mol Cell Biol.* 1999; 19:1990–1999. [PubMed: 10022886]
37. Cragle C, Macnicol AM. Musashi-directed translational activation of target mRNAs is mediated by the poly[A] polymerase, Germline Development-2. *J Biol Chem.* 2014

Developed a method for the synthesis of *E*-olefinic coupling products of PTL and MMB
Compounds screened for anticancer activity and effects on cell cycle progression
Two compounds showed good growth inhibitory effects on human cancer cell lines
The two compounds caused significant effects in oocyte maturation assays
Screening for effects on cell cycle progression complements cancer cell screening

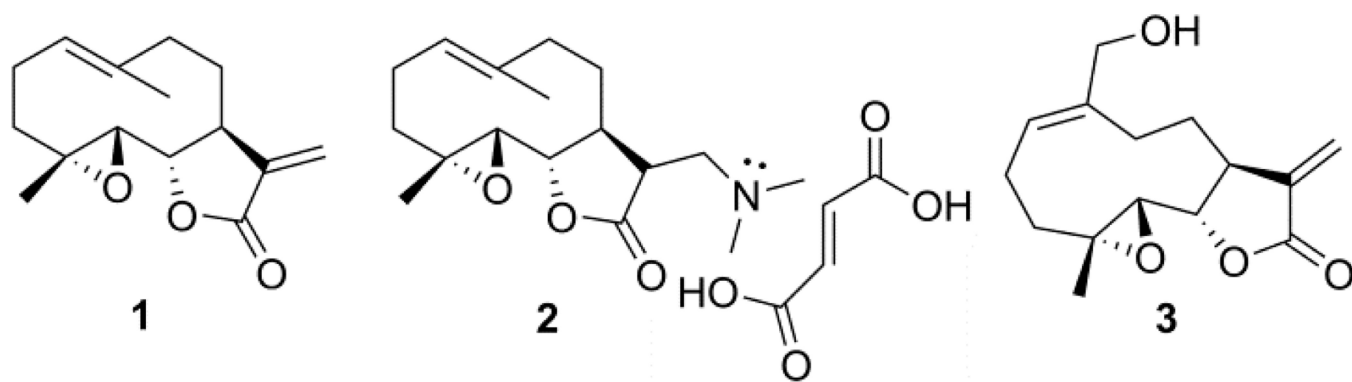


Fig 1.
Chemical structures of anti-leukemic sesquiterpene lactones (1–3).

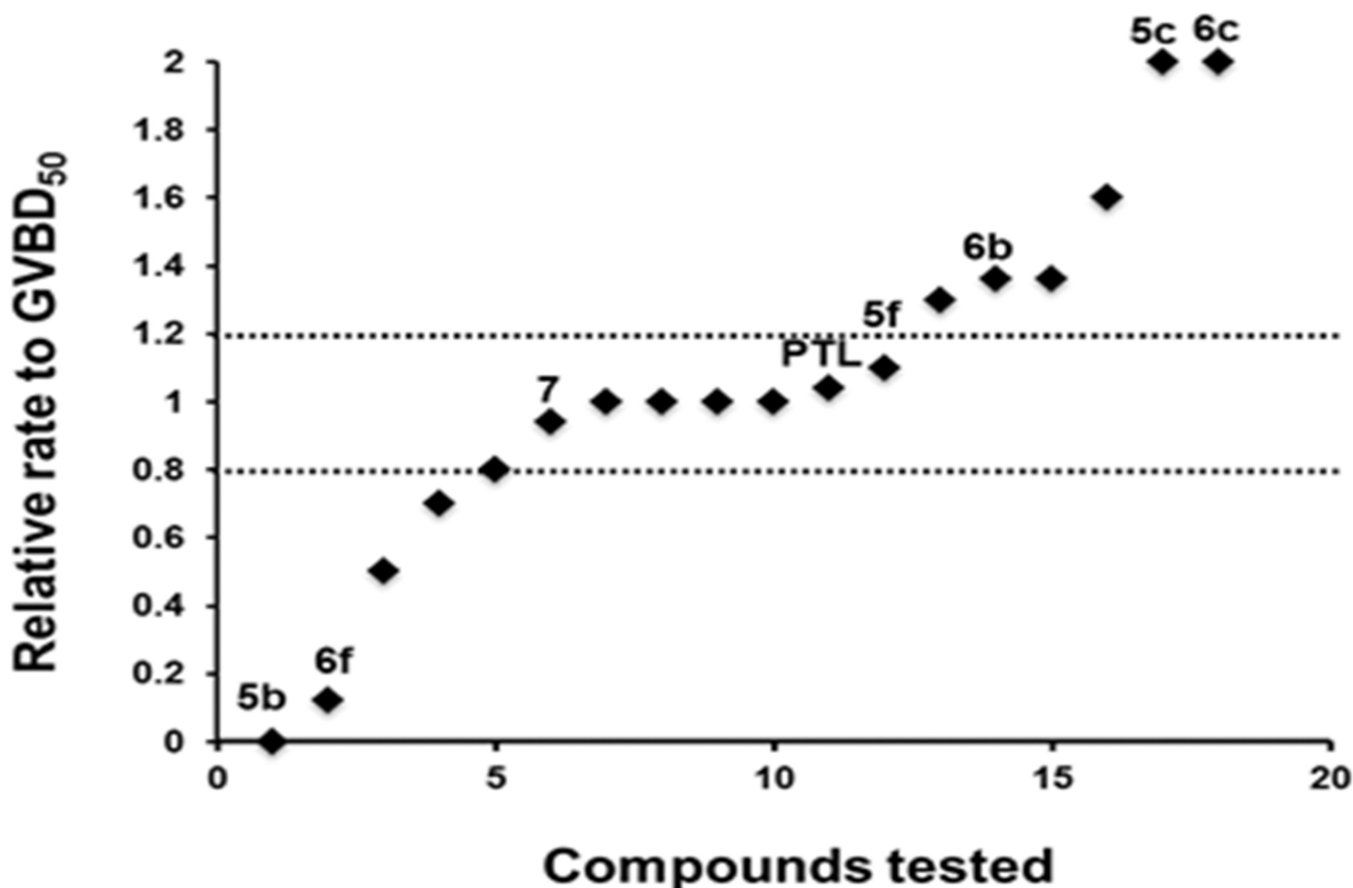


Fig. 2.

The rate of progression to GVBD was assessed for each test compound relative to the time taken for 50% of DMSO-treated control oocytes to complete GVBD (GVBD₅₀). A value of 1.0 indicates that the compound did not differ from DMSO-treated control oocytes. A value greater than 1.0 indicates an acceleration to maturation, with a value of 2.0 indicating spontaneous progression to GVBD without added progesterone. A value less than 1.0 indicates a delay to maturation, with a value of 0.0 indicating that no maturation occurred. Only compounds differing by more than 20% from DMSO-treated control oocytes were assessed further. Select compounds are identified by labels above their respective data point. Compounds **5c** and **6c** induced spontaneous maturation in the absence of added progesterone. Compounds **6b**, **6e**, **6g**, and **6i** accelerated progesterone-stimulated maturation by more than 20% relative to DMSO-treated controls. Compounds **5b** and **6f** were effective inhibitors of progesterone-stimulated maturation. None of the other compounds tested (including compounds **5f**, **7** and parthenolide (PTL)) exerted any reproducibly significant phenotypic effects upon progression to GVBD during oocyte maturation.

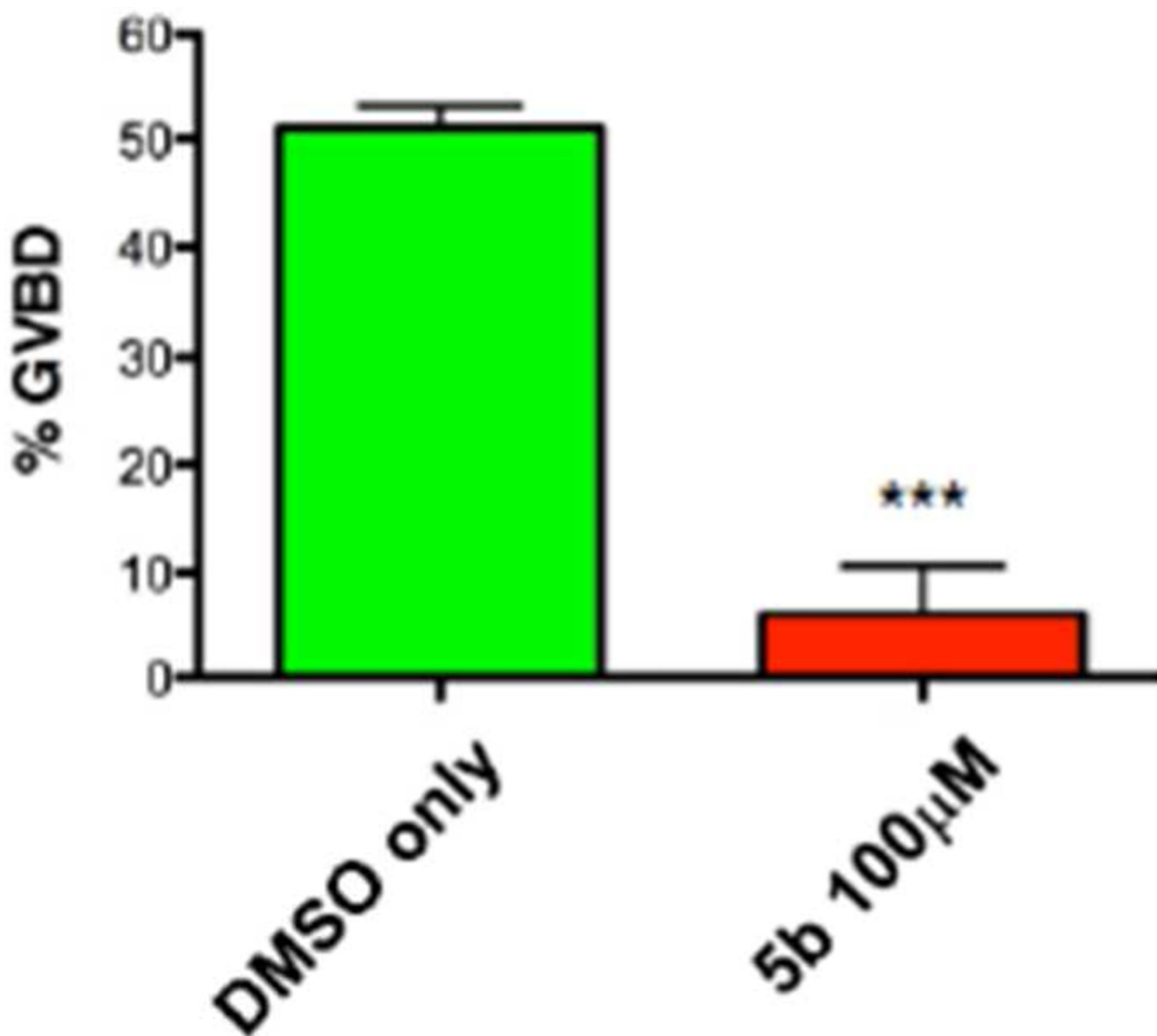


Fig. 3. Compound **5b** attenuates cell cycle progression in *Xenopus* oocytes. Oocytes were treated overnight with DMSO (vehicle) or 100 µM **5b**. The next morning, progesterone was added and the oocytes and the extent of maturation scored when 50% of DMSO-treated oocytes had completed GVBD. The results of three independent experiments are shown, Error bars represent S.E.M, $p < 0.001$, Student *t*-test.

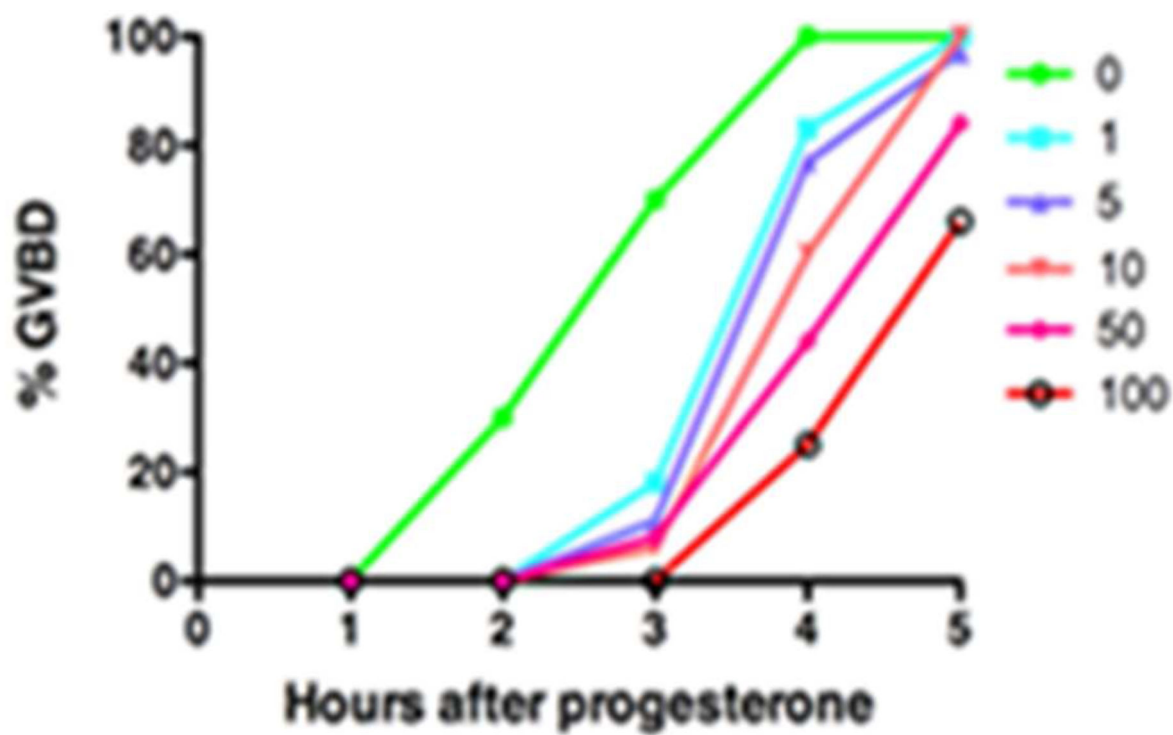


Fig. 4. Compound **5b** delays GVBD with increasing concentration (μM). Oocytes were treated overnight with DMSO (vehicle) or **5b** and then were stimulated the next morning with progesterone. The rate of progression through maturation was scored by the appearance of a white spot on the animal pole, indicative of GVBD.

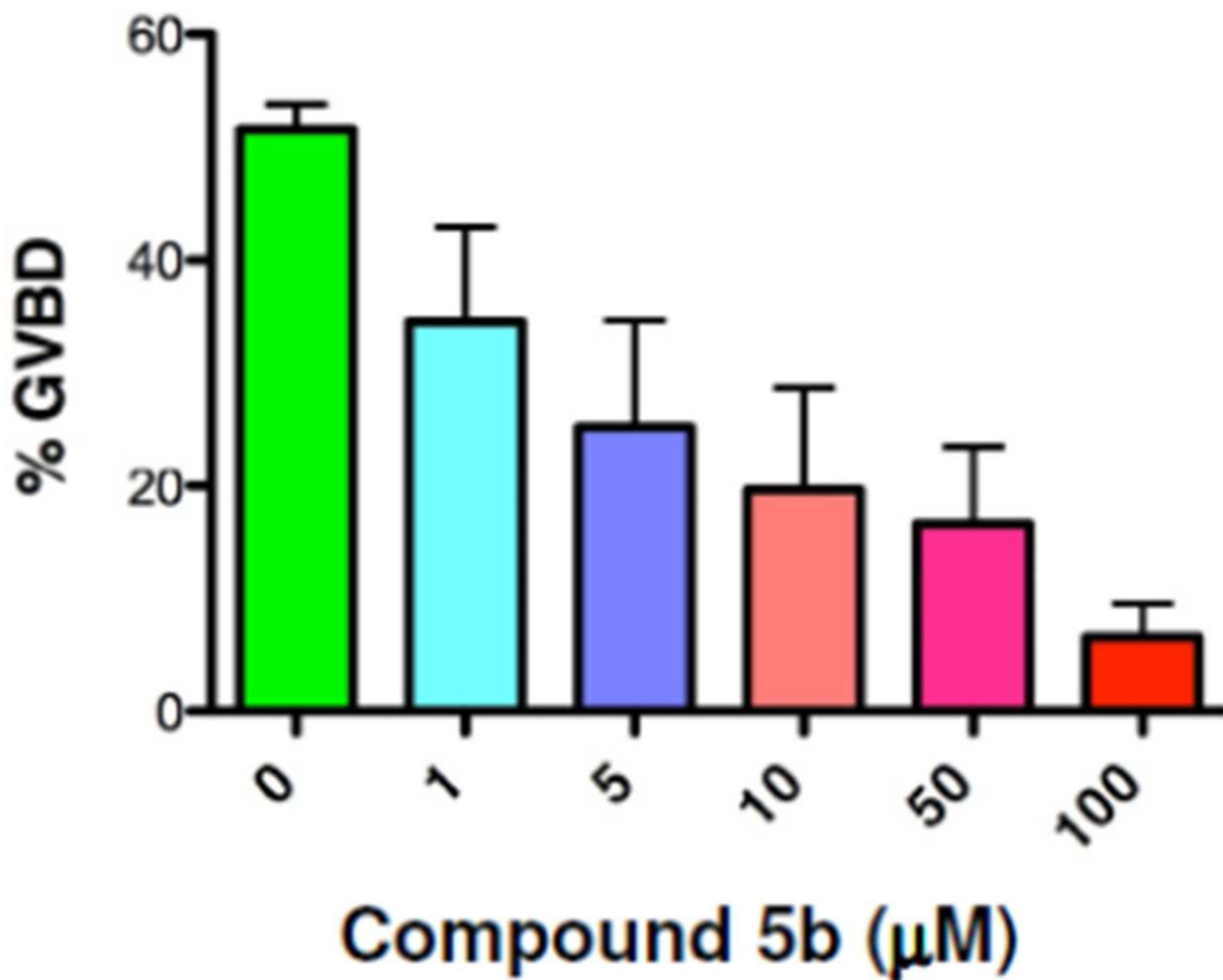


Fig 5. Compound **5b** attenuates cell cycle progression over a range of concentrations. Oocytes were treated overnight with DMSO (vehicle) or **5b** and then were stimulated the next morning with progesterone. The rate of progression through maturation was scored when 50% of the DMSO-treated control oocytes had completed GVBD. **5b** was found to inhibit progesterone-stimulated maturation with an EC_{50} of $5\mu\text{M}$. $n=5$, error bars represent S.E.M.

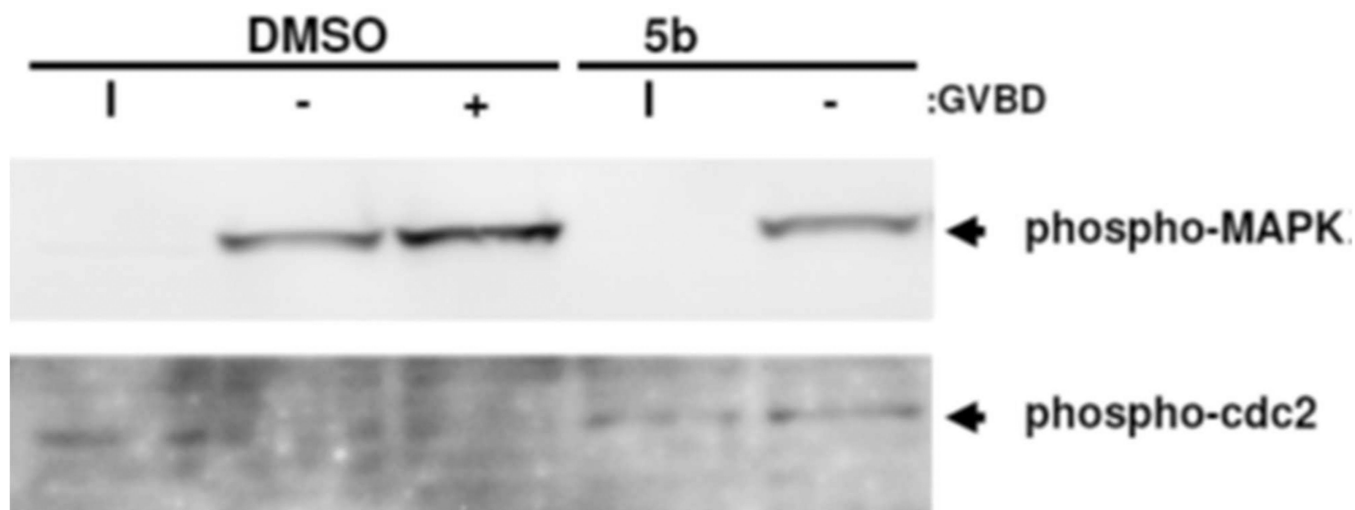


Fig. 6.

Compound **5b** signaling. Oocytes treated overnight with DMSO (vehicle) or **5b** were left unstimulated (I) or stimulated with progesterone. Oocytes were harvested when 50% of the DMSO oocytes reached GVBD and segregated into those that had not (–) or had (+) completed GVBD. Phospho-MAPK represents the activated form of the protein. Phospho-cdc2 reflects inactive MPF (cyclin B/CDK) protein.

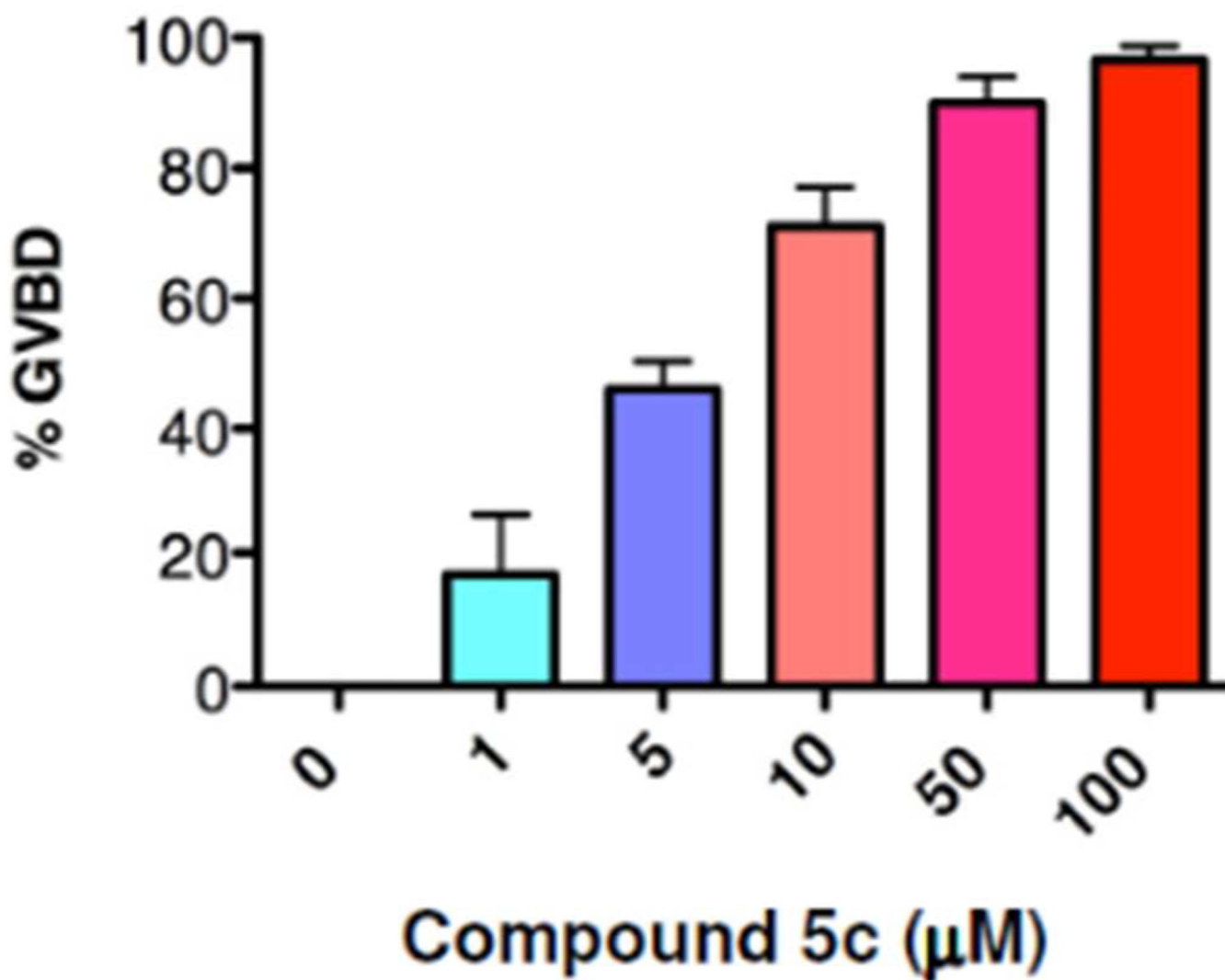


Fig 7. Compound **5c** induces progesterone-independent oocyte maturation. Oocytes were treated overnight with DMSO (vehicle) or compound **5c** and scored for maturation the next morning. **5c** induced oocyte GVBD with an EC_{50} of 6 μM . The combined results of 3 independent experiments are shown. Error bars represent S.E.M.

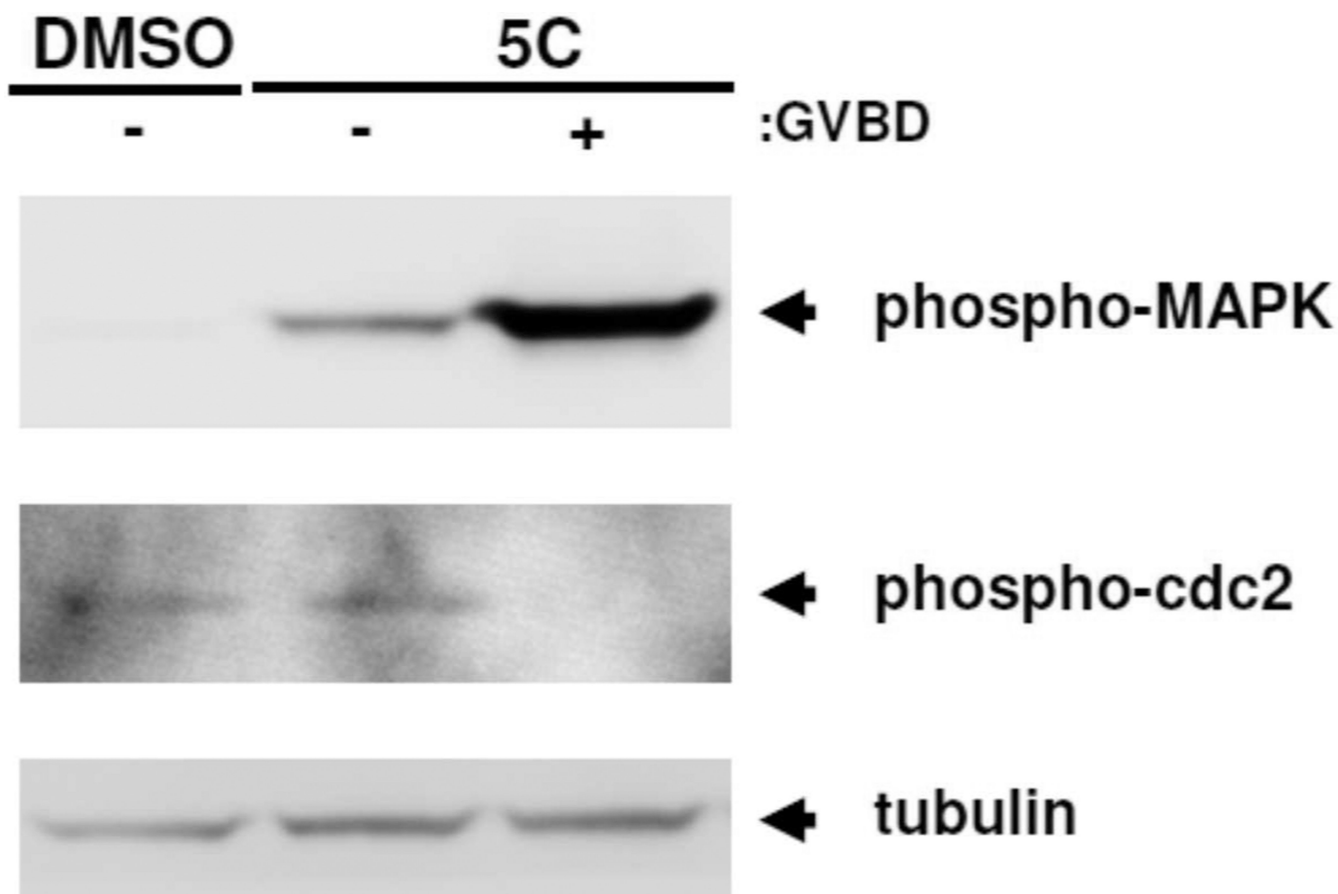
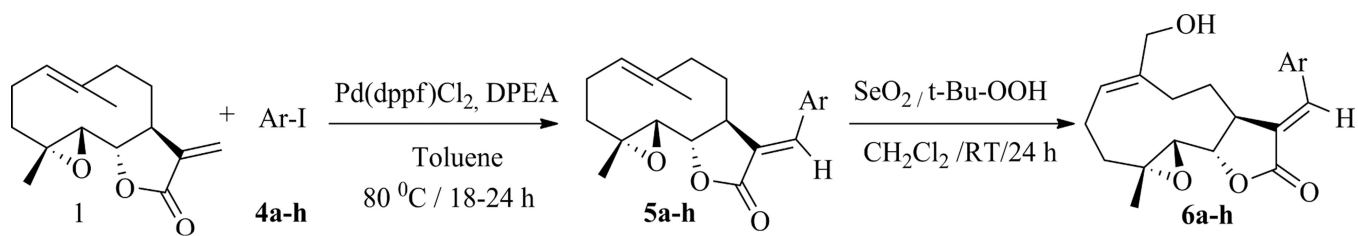
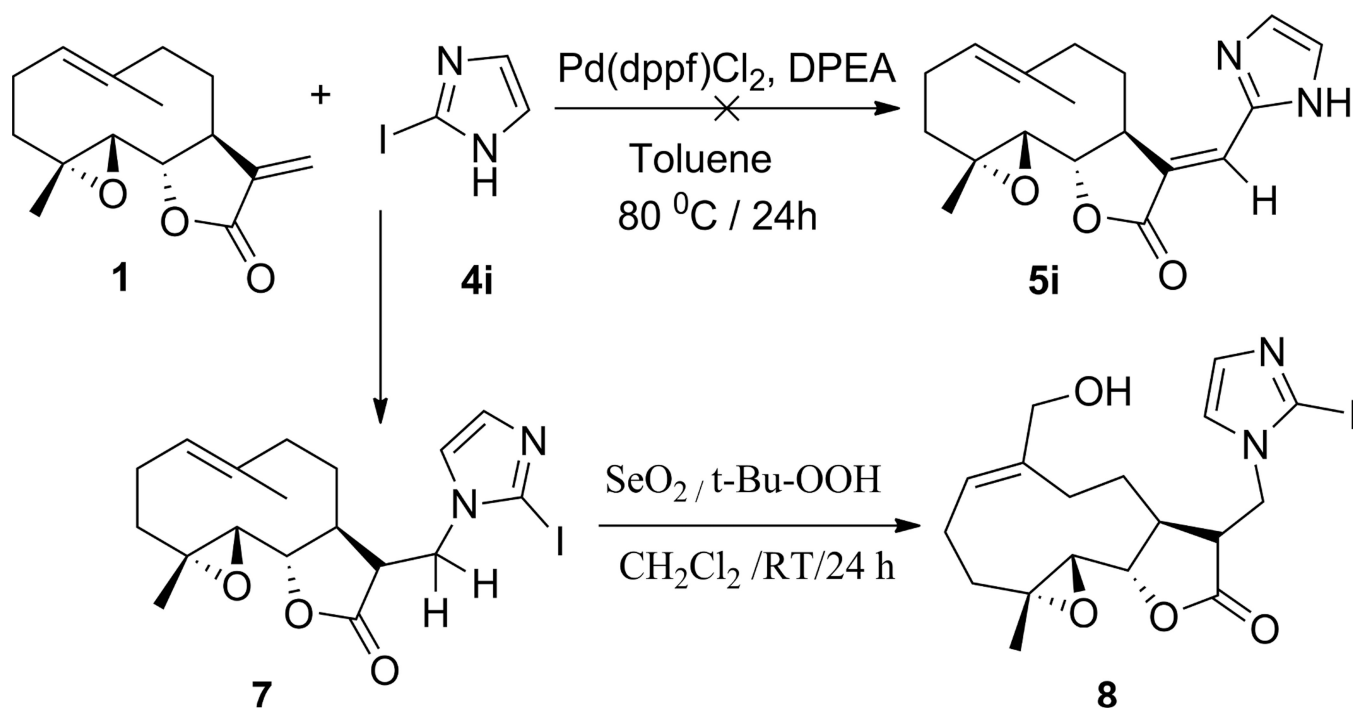


Fig. 8.

Compound **5c** signaling. Oocytes were treated with DMSO (vehicle) or compound **5c** and harvested when 50% of the compound **5c** oocytes completed GVBD. Compound **5c** treated oocytes were segregated into those that had not (-) or had (+) completed GVBD. **5c** triggered progesterone-independent activation of MAPK and MPF (visualized by dephosphorylation of cdc2). MAPK activation preceded GVBD, while cdc2 activation occurred at GVBD.

**Scheme 1.**

: Synthesis of *(E)*-13-(aryl/hetero aryl) analogs of PTL and MMB.



Scheme 2.

Reaction of parthenolide (1) with 2-iodoimidazole (4i) and subsequent oxidation of the product, 7, to the MMB analog 8.

Table 1

(E)-13-(aryl/hetero aryl) analogs of PTL (**5a–h**) and MMB (**6a–h**).

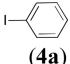
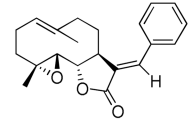
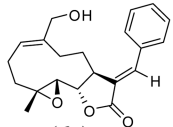
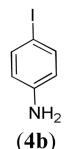
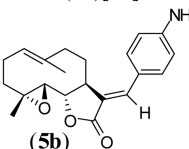
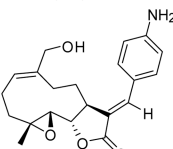
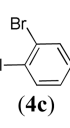
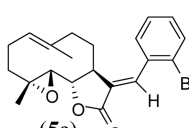
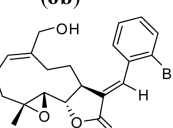
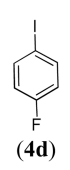
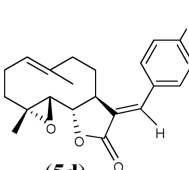
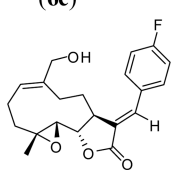
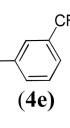
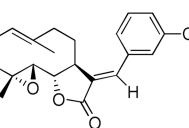
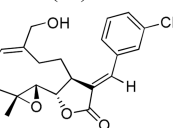
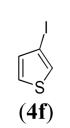
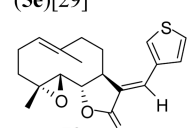
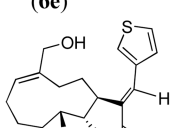
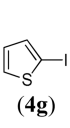
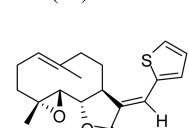
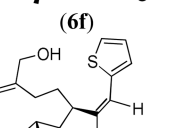
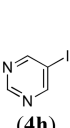
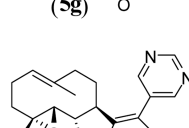
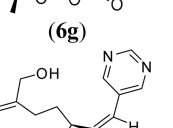
Ar-I	PTL-Heck products	MMB Heck analogs
 (4a)	 (5a) [29]	 (6a)
 (4b)	 (5b)	 (6b)
 (4c)	 (5c)	 (6c)
 (4d)	 (5d)	 (6d)
 (4e)	 (5e) [29]	 (6e)
 (4f)	 (5f)	 (6f)
 (4g)	 (5g)	 (6g)
 (4h)	 (5h)	 (6h)

Table 2

Antitumor activity (GI_{50} / μM)^a data of compounds **5f** and **7**; selected for 5 dose studies for the NCI 60-cell line screen

Panel/cell line	5f		7	
	GI_{50}	LC_{50} ^b	GI_{50}	LC_{50}
<u>Leukemia</u>				
CCRF-CEM	19.1	>100	6.13	79.6
HL-60(TB)	21.7	99.9	6.90	77.5
K-562	25.2	>100	7.36	90.0
MOLT-4	25.7	>100	19.6	97.9
RPMI-8226	19.7	>100	17.0	>100
SR	20.7	>100	13.6	>100
<u>Lung Cancer</u>				
A549/ATCC	29.8	>100	19.8	>100
HOP-62	35.8	>100	47.4	>100
NCI-H226	30.2	>100	15.4	62.3
NCI-H23	23.0	>100	23.7	>100
NCI-H322M	44.7	>100	61.3	>100
NCI-H460	29.3	>100	30.1	>100
NCI-H522	5.44	59.7	1.71	6.34
<u>Colon Cancer</u>				
COLO 205	22.6	90.9	14.5	58.8
HCC-2998	33.8	>100	NA	NA
HCT-116	28.3	>100	11.8	49.0
HCT-15	22.6	>100	10.7	55.6
HT29	27.0	>100	17.6	61.5
KM12	20.4	86.7	43.2	>100
SW-620	22.9	>100	11.4	62.8
<u>CNS Cancer</u>				
SF-268	21.3	>100	23.0	>100
SF-295	28.5	>100	32.1	>100
SF-539	16.1	62.2	16.7	60.8
SNB-19	47.6	>100	>100	>100
SNB-75	21.5	>100	19.3	>100
U251	21.7	>100	36.7	>100
<u>Melanoma</u>				
LOX IMVI	18.0	71.2	14.9	60.9
MALME-3M	22.5	>100	10.9	62.7
M14	20.5	>100	16.5	65.6
MDA-MB-435	18.3	>100	13.8	59.5
SK-MEL-2	NA	NA	18.6	66.1

Panel/cell line	5f		7	
	GI ₅₀	LC ₅₀ ^b	GI ₅₀	LC ₅₀
SK-MEL-28	29.4	>100	16.1	73.0
SK-MEL-5	16.3	60.4	18.5	95.6
UACC-257	16.6	>100	12.0	53.9
UACC-62	13.8	76.6	NA	NA
<u>Ovarian Cancer</u>				
IGROV1	27.9	>100	20.0	75.6
OVCAR-3	20.5	>100	6.85	50.8
OVCAR-4	24.3	>100	13.2	60.0
OVCAR-5	48.1	>100	13.7	52.5
OVCAR-8	26.9	>100	16.6	59.9
NCI/ADR-RES	23.6	>100	31.2	>100
SK-OV-3	44.9	>100	47.3	>100
<u>Renal Cancer</u>				
786-0	35.7	>100	14.3	53.0
A498	17.5	>100	45.2	>100
ACHN	32.8	>100	10.5	47.4
CAKI-1	30.9	>100	6.61	49.5
RXF 393	18.1	>100	NA	NA
SN12C	25.8	>100	17.7	84.1
TK-10	34.7	>100	NA	NA
UO-31	27.3	>100	10.8	50.0
<u>Prostate Cancer</u>				
PC-3	22.7	>100	23.1	>100
DU-145	25.7	>100	18.8	68.3
<u>Breast Cancer</u>				
MCF7	20.0	>100	9.79	>100
MDA-MB-231/ATCC	16.0	81.8	16.4	59.6
HS 578T	21.5	>100	21.3	>100
BT-549	20.1	88.2	15.9	55.3
T-47D	29.5	>100	9.88	54.3
MDA-MB-468	17.7	>100	11.1	60.4

na: Not analyzed;

^a GI₅₀: 50% Growth inhibition, concentration of drug (μM) resulting in a 50% reduction in net cell growth as compared to cell numbers on day 0.

^b LC₅₀ the drug concentration (μM) that was required to kill 50% of the cells.